Excitation Transfer in Helium†

R. B. KAY* AND R. H. HUGHES
Physics Department, University of Arkansas, Fayetteville, Arkansas
(Received 6 July 1966; revised manuscript received 15 September 1966)

The apparent lifetimes of the n^1P, 3^1D, 4^1D, and 3^3D levels of helium are studied as a function of pressure. The collisional transfer of excitation from n^1P levels to nF levels is conclusively shown to be an important mechanism in populating D levels. It is found that the Wigner spin rule inhibits collisional transfer between 4^1P and 4^3F levels. For $n>4$, the n^1P transfer to n^3F levels is about three times greater than to the n^1F levels. For $n>4$, the cross sections for collisional transfer from nF to n^1P levels are found to be about 10% of those for the reverse process. This result is in agreement with the principle of detailed balance. The collisional $n^1P \rightarrow nF$ transfer cross sections are measured and appear to increase approximately as n^4. The pressure dependence of the apparent $3D$ cross sections are calculated, using the above measurements in conjunction with the $n^1P \rightarrow nF$ transfer model. The results are found to be in excellent agreement with experimental measurements.

I. INTRODUCTION

THE problem of collisional transfer of ^1P level excitation to D levels in helium has been a subject of interest since its discovery by Lees and Skinner[1] in 1930. An extensive study by Maurer and Wolf[2] decisively showed the existence of this mechanism and the following reaction was proposed:

$$\mathrm{He}(n^1P)+\mathrm{He}(1^1S) \rightarrow \mathrm{He}(1^1S)+\mathrm{He}(n^{3,1}D).$$

Although able to account for the experimental findings, this reaction violates the Wigner conservation-of-spin rule in the case of transfer to n^3D states.

Heron *et al.*[3] (1956) showed from measurement of the lifetime of the 3^1P level that collisional transfer can have little effect on the population of this level. It can be concluded that the above reaction is unimportant at $n=3$. In a study of excitation mechanisms in helium, Gabriel and Heddle[4] found that the ratio of the collisional population of the n^3D to n^1D levels tends towards 3 to 1 at high pressures which is the ratio of their statistical weights. They further concluded that cascade (radiative transfer) played an important role in the process. St. John and Fowler[5] followed by proposing the two-step reaction

$$\mathrm{He}(n^1P)+\mathrm{He}(1^1S) \rightarrow \mathrm{He}(n^{1,3}F)+\mathrm{He}(1^1S)$$
$$\mathrm{He}(nF) \rightarrow \text{cascade} \rightarrow \mathrm{He}(n'D), \quad n>n'.$$

Lin and Fowler[6] gave theoretical support to this hypothesis by showing that spin is not necessarily a constant of the motion for F levels. Further, they show that $\Delta L=\pm 2$ is favored in such collisions. Pendleton and Hughes[7] and Fowler *et al.*[8] have reported cascading components in the $3^3D \rightarrow 2^3P$ decay. The lifetimes of these components suggested nF level decay in support of the $nP \rightarrow nF$ transfer model.

St. John and Nee[9] have used recent absolute electron-impact cross-section measurements along with the $n^1P \rightarrow nF$ transfer model in an attempt to explain the pressure dependence of the apparent cross-section curves for the n^3D and n^1D levels. However, they assumed that the n^1P transfer to $^3F_3$ and $^1F_3$ states is weighted equally, with $^3F_{2,4}$ states not taking part. (It is not evident that the collision process should be so selective.) They further assumed that the spin-conservation rule is completely violated for all n.

In this investigation we have made use of time-resolved spectroscopy in order to study the collision process. The apparatus is essentially that described in Ref. 7. A gated, variable-energy electron beam provides the necessary excitation. The beam is gated on for a period sufficient for equilibrium to be established and then is gated off. The decay rates of the excited state of interest is measured by monitoring the intensity of an appropriate spectral line. The apparatus uses a sampling method of detection. Presently a dc-operated Amperex 56AVP photomultiplier is being used. The apparatus has been modified for electronic logarithmic readout to facilitate a study of multimode decay schemes. Spectral isolation is accomplished by using either a Bausch and Lomb 500-mm monochromator with an inverse dispersion of 17 Å/mm or by using Baird-Atomic B-1 interference filters. The electron beam is a sheet beam having approximate dimensions of 3 mm by 15 mm. Pressures were measured with a McLeod-calibrated Pirani gauge.

In all of the past collisional-transfer studies, no direct measurements of the n^1P collisional transfer cross sections have been obtained. We have succeeded in

† Work supported by the National Science Foundation.
* Present address: Physics Department, University of Florida, Gainesville, Florida.
[1] J. H. Lees and H. W. B. Skinner, Proc. Roy. Soc. (London) **A137**, 186 (1932).
[2] W. Maurer and R. Wolf, Z. Physik **115**, 410 (1940).
[3] S. Heron, R. W. P. McWhirter, and E. H. Rhoderick, Proc. Roy. Soc. (London) **A134**, 564 (1956).
[4] A. H. Gabriel and D. W. O. Heddle, Proc. Roy. Soc. (London) **A258**, 124 (1960).
[5] R. M. St. John and R. G. Fowler, Phys. Rev. **122**, 1813 (1961).
[6] C. C. Lin and R. G. Fowler, Ann. Phys. (N. Y.) **15**, 461 (1961).
[7] W. R. Pendleton and R. H. Hughes, Phys. Rev. **138**, A683 (1965).
[8] R. G. Fowler, T. M. Holtzberlein, C. H. Jacobson, and S. J. B. Corrigan, Proc. Phys. Soc. (London) **84**, 539 (1964).
[9] R. M. St. John and Tsu-Wei Nee, J. Opt. Soc. Am. **55**, 426 (1965).

performing such measurements by studying the lifetimes of n^1P levels as a function of pressure. From these measurements, we are able to infer the cross sections for collisional transfer. Several of the cascading F-level contributions to the population of the 3^3D and 3^1D levels are time resolved in the $3D$ decay. We are thus able to follow the collision process from level to level. From our work we conclude that there is little doubt that the $n^1P \rightarrow nF$ transfer model is correct.

II. TREATMENT OF DATA

A. Coupled P and F States

Let us define ${}^1\sigma_1$, ${}^3\sigma_1$, and $\sigma_1={}^1\sigma_1+{}^3\sigma_1$ to be the cross sections for $n^1P \rightarrow n^1F$, $n^1P \rightarrow n^3F$, and total $n^1P \rightarrow nF$ transfer, respectively. Further, we let ${}^1\sigma_2$ and ${}^3\sigma_2$ be the cross section for back transfer $n^1F \rightarrow n^1P$ and $n^3F \rightarrow n^1P$, respectively. The relative sizes of these transfer cross sections can be obtained by appealing to the principle of detailed balance. Thus

$$3\,{}^1\sigma_1=7\,{}^1\sigma_2, \quad 3\,{}^3\sigma_1=21\,{}^3\sigma_2,$$

and

$$({}^3\sigma_1)({}^1\sigma_1)^{-1}=3({}^3\sigma_2)({}^1\sigma_2)^{-1}=B, \tag{2.1}$$

where B is the branching ratio for ^1P transfer to the ^3F and ^1F systems. It follows that

$${}^1\sigma_2=\frac{3}{7(1+B)}\sigma_1$$

and

$${}^3\sigma_2=\frac{B}{7(1+B)}\sigma_1.$$

For the F-state systems where total spin is no longer conserved, then

$${}^3\sigma_2={}^1\sigma_2=\sigma_2=(3/28)\sigma_1 \tag{2.2}$$

and $B=3$. Experimentally, we conclude that $B=3$ for $n>4$. For such systems, the population of the ^1P and F levels can be described by two coupled first-order linear equations. For a given principal quantum number and after cessation of the electron pulse, these equations are

$$\dot{n}_p=-n_p(A_p+\rho v\sigma_1)+n_f\rho v\sigma_2, \tag{2.3}$$

$$\dot{n}_f=-n_f(A_f+\rho v\sigma_2)+n_p\rho v\sigma_1, \tag{2.4}$$

where n_p is the density of atoms in the ^1P level, n_f is the density of atoms in the F levels, ρ is the gas density (atoms/cm^3), v is the mean relative thermal velocity (1.78×10^5 cm/sec), A_f is the total radiative transition probability for the F level (which is the same for a n^3F or a n^1F level), and A_p is the "imprisoned" total radiative transition probability for the ^1P level.

A_p is given by $A_p=A_s+gA_1$, where A_s is the sum of the transition probabilities for the P-state decay to levels other than the ground state, and A_1 is the transition probability for decay to the ground state. The factor g gives the fraction of resonance quanta which escape absorption in the collision chamber and is a function of the resonance absorption coefficient k and the effective chamber radius r. The average value of g as a function of kr, which has been calculated by Phelps[10] and plotted by Gabriel and Heddle,[4] is used in the analysis of the ^1P series. All transition probabilities are taken from Ref. 4.

The solutions to the rate equations are

$$n_p(t)=C_1e^{m^-t}+C_2e^{m^+t}, \tag{2.5}$$

and

$$n_f(t)=C_3e^{m^-t}+C_4e^{m^+t}, \tag{2.6}$$

where

$$m^{\pm}=\frac{1}{2}\Big\{-(A_p+\rho v\sigma_1+A_f+\rho v\sigma_2) \pm(A_p+\rho v\sigma_1-A_f-\rho v\sigma_2) \times\left(1+\frac{4\rho^2v^2\sigma_1\sigma_2}{(A_p+\rho v\sigma_1-A_f-\rho v\sigma_2)^2}\right)^{1/2}\Big\}. \tag{2.7}$$

Since $\sigma_2/\sigma_1\approx1/10$, we expand and neglect terms in $(\sigma_2)^2(\sigma_1)^{-2}$ and the higher orders with the result, for $A_p>A_f$,

$$m^+=-(A_f+K_+\rho v\sigma_2), \tag{2.8}$$

$$m^-=-(A_p+\rho v\sigma_1+K_-\rho v\sigma_2), \tag{2.9}$$

where $0<K_+<1$ and $1>K_->0$ with $K_+\approx0$, $K_-\approx1$ when $\rho v\sigma_1\gg(A_p-A_f)$ and $K_+\approx1$, $K_-\approx0$ when $\rho v\sigma_1 \ll(A_p-A_f)$. The decay of the ^1P level and the F levels will exhibit characteristics of both systems. The usually faster m^- component will be closely associated with P-state decay while the m^+ component is closely associated with the F-state decay. It is interesting to note that setting $K_-=0$ will make at most a 10% error in m^-. Since our accuracy is no better than this, we make this approximation in evaluating σ_1 from the P-state lifetimes.

B. Cascade Correction

Consider the case where a level k cascades to a level j. The rate equation for level j is

$$\dot{n}_j=\Phi\rho Q_j+n_kA_{kj}-n_jA_j, \tag{2.10}$$

where n_j and n_k are the atom densities in the respective states, Q_j is the cross section for populating j by direct electron impact, Φ is the electron flux, ρ is the gas density, A_j is the total radiative transition probability for j decay and is the reciprocal of the radiative mean lifetime τ_j, and A_{kj} is the radiative probability for $k \rightarrow j$ decay. If the excitation pulse width is sufficiently long, then equilibrium will be established. Under these conditions when the electron beam is then turned off

[10] A. V. Phelps, Phys. Rev. **110**, 1362 (1958).

at $t=0$, the density of atoms in state j is

$$n_j^0=(\Phi\rho Q_j+n_k^0A_{kj})\tau_j. \quad (2.11)$$

For $t>0$, $\Phi=0$ and $n_k=n_k^0e^{-t/\tau_k}$, then

$$n_j=\beta e^{-t/\tau_j}+\gamma_k e^{-t/\tau_k}, \quad (2.12)$$

where $\gamma_k=n_k^0A_{kj}(A_j-A_k)^{-1}$, $A_k=\tau_k^{-1}$, and $\beta=n_j^0-\gamma_k$.

The coefficient β of e^{-t/τ_j} is the magnitude of this decay-component intercept at $t=0$. One sees that this is not equal to the density of atoms initially in state j. Alternatively, $\beta=n_j^*-\gamma_k\tau_j/\tau_k$, where $n_j^*=\tau_j\Phi\rho Q_j$ is the density of atoms placed in state j by direct electron impact in the absence of cascade. The actual density of atoms placed by direct electron excitation in state j, n_j^*, can thus be obtained from the intercepts β and γ_k. If there are several cascading levels present, then it is necessary to sum over k.

The apparent electron-impact cross section Q_j' is customarily defined through the equation $n_j^0=\tau_j\Phi\rho Q_j'$. It follows that

$$Q_j'=Q_j[1+(\Phi\rho Q_j)^{-1}\textstyle\sum_k n_k^0A_{kj}]. \quad (2.13)$$

We now identify the level j with the $3D$ levels in helium and the k level with F levels. The k (i.e., F) states will decay with nearly their radiative lifetimes as shown by the result, $m^+\approx -A_f$. We assume that the population of F states by direct electron impact is negligible in our energy range, an assumption which is supported by Born-approximation calculations and the success of our fit with such a model.

The complete rate equations, neglecting cascade as a populating mechanism, for a given principal quantum number are

$$\dot{n}(^1P)=-(A_p+\rho v\sigma_1)n(^1P)+{}^1\sigma_2\rho vn(^1F)+{}^3\sigma_2\rho vn(^3F)+\Phi\rho Q(^1P), \quad (2.14)$$

$$\dot{n}(^1F)=-(A_f+{}^1\sigma_2v\rho)n(^1F)+{}^1\sigma_1v\rho n(^1P), \quad (2.15)$$

$$\dot{n}(^3F)=-(A_f+{}^3\sigma_2v\rho)n(^3F)+{}^3\sigma_1v\rho n(^1P). \quad (2.16)$$

Setting $\dot{n}(^1P)=\dot{n}(^1F)=\dot{n}(^3F)=0$ allows us to obtain the equilibrium F-state densities, $n(^1F)^0$ and $n(^3F)^0$.

For the case of complete LS coupling breakdown, ${}^3\sigma_2={}^1\sigma_2$ and we may write

$$Q'(^iD)=Q(^iD)\{1+\textstyle\sum_n(^i\alpha)Q(n^1P)\times[Q(^iD)]^{-1}f_n(\rho)\}, \quad (2.17)$$

where $i=1$ or 3 according to whether in the singlet or triplet system, ${}^1\alpha=\frac{1}{4}$, ${}^3\alpha=\frac{3}{4}$, and

$$f_n(\rho)=\frac{\sigma_1(n)\rho vA(nf\rightarrow 3D)}{A_p(n)[A_f(n)+\rho v\sigma_2(n)]+A_f(n)\rho v\sigma_1(n)}. \quad (2.18)$$

Thus, $f_n(\rho)$ is a measure of the fraction of direct n^1P excitation which ends up as $3D$ excitation.

We define

$$F_n^i(\rho)=(^i\alpha)Q(n^1P)[Q(^iD)]^{-1}f_n(\rho). \quad (2.19)$$

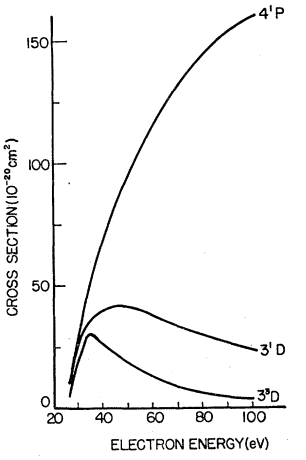

FIG. 1. Apparent cross sections for exciting the 4^1P, 3^1P, and 3^3D levels by electron impact based on measurements by St. John, Miller, and Lin (Ref. 11).

In the case where the spin-conservation rule has some validity, then ${}^3\sigma_2\neq{}^1\sigma_2$ and $F_n^i(\rho)$ is of a somewhat different form which can be obtained in terms of the branching ratio B. We find this to be the case only for $n=4$ and thus $F_4^i(\rho)$ is determined separately. We let

$$F^i(\rho)=F_4^i(\rho)+\textstyle\sum_{n=5}F_n^i(\rho). \quad (2.20)$$

Thus

$$Q'(^iD)=[1+F^i(\rho)]Q(^iD). \quad (2.21)$$

III. RESULTS

The n^1P, 3^3D, and 3^1D levels of helium were extensively studied. The 4^1D and 3^3P levels were also investigated but to a lesser extent. Excitation pulse lengths were varied from 50 nsec to 2 μsec according to the lifetimes of the involved decays. All levels except the 3^3D and 3^1D levels were investigated, using only the monochromator for spectral isolation.

It is helpful to have in mind the shape of the excitation functions of the various levels studied. In Fig. 1, representative functions for ^1P, ^1D, and ^3D levels are given by the 4^1P, 3^1D, and 3^3D cross sections versus energy as measured by St. John *et al.*[11] One can enhance the characteristics of a given level by selecting the energy at which its cross section maximizes. Although the 3^3D level peaks at 35 eV, it was found that the current from the electron gun at 38 eV was sufficiently more to warrant using this potential.

A. The n^1P Series

The lifetimes of the n^1P levels as a function of pressure were studied using 100-eV excitation.

1. The 3^1P Level

The 3^1P level was observed via the $3^1P\rightarrow 2^1S$ (λ 5015 Å) radiation. The decay was found to be essentially a pure exponential. Departure from a single

[11] R. M. St. John, F. L. Miller, and C. C. Lin, Phys. Rev. **134**, A888 (1964).

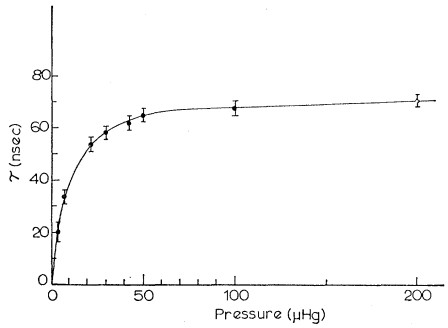

FIG. 2. Lifetime of the 3^1P level as a function of pressure. (Error bars indicate average deviations.)

exponential is estimated as no more than 2% at 200-μ Hg pressure. The lifetime of this level vs pressure is shown in Fig. 2. The smooth curve through the data points is given by an imprisoned lifetime calculation using an imprisonment radius of 1.31 cm. This imprisonment radius was taken as a constant for our chamber and was used to calculate the imprisoned lifetimes of the other members of the n^1P series.

2. The 4^1P Level

This level was studied via the $4^1P \rightarrow 2^1S$ (λ 3965 Å) line.

The decay of the 4^1P level was found to be essentially a pure exponential at pressures below 50 μ Hg where departure from a single exponential was 5% or less. At a pressure of $\sim$200 μ Hg, a long-lived component, which appeared to have a lifetime around 150 nsec, contributed about 15% to the decay scheme. The fast, dominant component was assumed to be collisionally shortened 4^1P decay. The lifetime of this component can be expressed as $(A_p+\rho v\sigma_1)^{-1}$. The smooth curve through the data points in Fig. 3 is given by this expression with $\sigma_1=2\times10^{-14}$ cm^2. Also shown is the calculated imprisonment lifetime, $(A_p)^{-1}$, to show the marked effect of collisional transfer on the 4^1P lifetime.

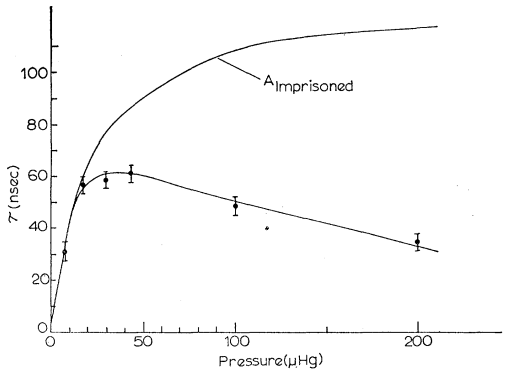

FIG. 3. Lifetime of the 4^1P level as a function of pressure. Curve labeled "A imprisoned" is the lifetime expected without collisional effects. (Error bars indicate average deviations.)

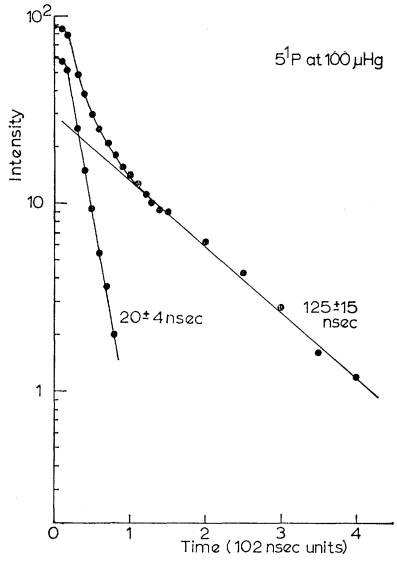

FIG. 4. Typical 5^1P level decay scheme at 100 μ Hg. The fast component is associated with collisionally shortened 5^1P lifetime while the long-lived component is attributed to 5^1F level back transfer to the 5^1P level.

3. The 5^1P and 6^1P Levels

These levels were studied via the $5^1P \rightarrow 2^1S$ (λ 3614 Å) and the $6^1P \rightarrow 2^1S$ (λ 3448 Å) lines. They show a definite two-component decay as predicted in Sec. IIA for coupled P and F systems. Figure 4 gives the decay scheme of the 5^1P level at 100 μ Hg. It is typical of the decay schemes for these levels. The lifetime of the long-lived component in the 5^1P decay is near that of the 5^1F lifetime, and the lifetime of the long-lived component in the 6^1P decay is near that of the 6^1F lifetime. The long-lived components become an increasingly larger fraction of the decay as pressure is increased.

Figures 5 and 6 show the pressure dependency of the lifetimes of the fast components. The fast-component lifetimes were interpreted as collisionally shortened ^1P lifetimes. The smooth curves through the data points in Figs. 5 and 6 were calculated with $\sigma_1=6.4\times10^{-14}$ cm^2 and 13×10^{-14} cm^2 for the 5^1P and 6^1P states, respectively.

B. The D Levels

In the study of $3D$ radiation, advantage was taken of the increased optical speed afforded by a system using interference filters. The field stop of the system was the cathode of the photomultipler. A unit-magnification lens system imaged the entrance window in the center of the chamber. The diameter of the photocathode was considerably larger than the width of the electron beam. As a consequence, more light produced by the atom-atom collisions in the resonance halo was detected relative to the light produced by direct electron impact than would be the case if the field stop were more restrictive. In most electron-excitation cross-section measurements, the optical field of view is limited to the immediate area of the electron beam. The photon yield

into the known solid angle subtended by the optical system is measured, and a simple correction is applied to obtain the yield into a 4π solid angle. The effect of the increased field of view in the filter system had to be determined.

Although the lifetime apparatus is designed for dynamic measurements, the electron beam can be operated in a dc mode. The apparatus was fitted with a suitable Faraday cup to measure the electron current in order that excitation functions could be determined for $3^3D \rightarrow 2^3P$ (λ 5876 Å) line, using either the filter system or the monochromator for spectral isolation. The intensity per unit current at a constant pressure was measured as a function of the electron energy. The shape of the excitation function is very pressure sensitive. Since a good portion of the excitation can come from ^1P transfer, the resulting excitation function is a sum of an excitation function for direct 3^3D electron impact excitation and an excitation function for the n^1P levels. The 3^3D excitation function was measured at 10-μ Hg pressure with the filter system and with the monochromator system. The monochromator slits were adjusted to restrict the field of view to the immediate area of the electron beam. The two excitation functions were considerably different. This is to be expected in view of the strikingly different excitation functions for the directly excited 3^3D level and the n^1P levels of which the 4^1P level is assumed representative (Fig. 1).

The apparent relative cross section versus energy (excitation function) was assumed to have the form

$$Q'(3^3D)=Q(3^3D)+RQ(4^1P),$$

where R is a single-valued but adjustable parameter required to fit the excitation function. Figure 7 shows that both the excitation functions could be fitted quite well with the above relationship. The value of R required to fit the filter curve was 3 times that required for the monochromator curve. In view of this result, the expression (2.21) is modified to include a field-of-view factor Ω for our apparatus. The expression becomes

$$Q'(^iD)=[1+\Omega F^i(\rho)]Q(^iD),$$

where $\Omega=1$ when the field of view is suitably restricted and $\Omega=3$ for measurements with the filter system. (Ω and R depend on the size of the entrance window.)

It is true that this correction would have been unnecessary if we had restricted the field of view of the filter system, but it is felt that the additional signal obtained by not restricting the field warranted this procedure. A comparison of the time-resolved 3^3D decay using the monochromator and the filter system also verified the factor 3 within the experimental error.

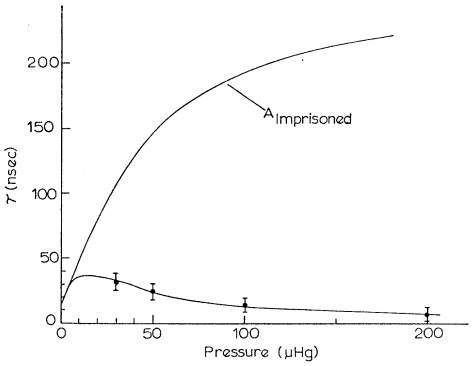

FIG. 5. Lifetime of the fast component in the 5^1P decay as a function of pressure. The curve labeled "A imprisoned" is the 5^1P level lifetime expected without collisional effects. (Error bars indicate estimated limit errors.)

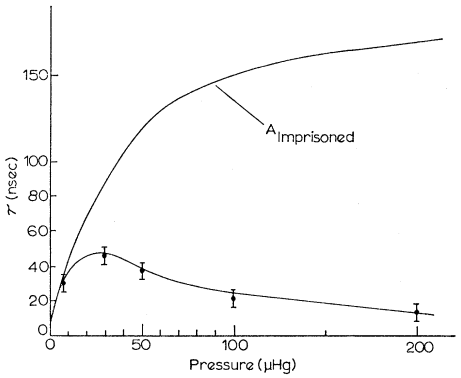

FIG. 6. Lifetime of the fast component in the 6^1P decay as a function of pressure. Curve labeled "A imprisoned" is the 6^1P level lifetime expected without collisional effects. (Error bars indicate estimated limit errors.)

1. The 3^3D Level

The decay scheme for the $3^3D \rightarrow 2^3P$ transition at 34-μ Hg pressure after 38-eV excitation is given in Fig. 8. This composite curve is broken down into lifetimes of 15, 70, 144, 260, and 700 nsec. The first three closely correspond to the theoretical lifetimes of the 3^3D, 4^3F, and 5^3F levels, respectively. The 260-nsec decay is very close to the theoretical 6^3F lifetime but probably includes some of the 7^3F (350 nsec) decay. The importance of the 6^3F level to the total decay may then be overestimated. The ~700 nsec decay is presumed to be a composite of n^3F lifetimes for higher values of n.

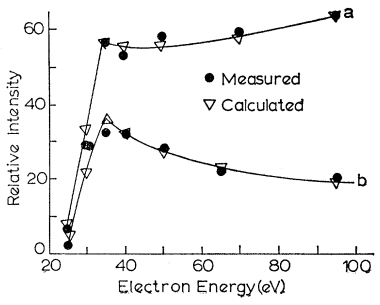

FIG. 7. Excitation functions for the 3^3D level at 10 μ Hg. Curve a is the 3^3D excitation calculated for and measured by the filter system. Curve b represents observations with the monochromator.

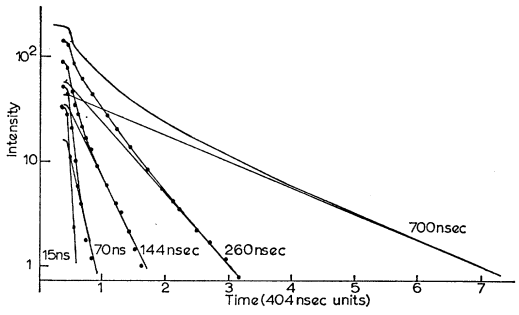

FIG. 8. Decay scheme of the 3^3D level at a pressure of 34 μ Hg after 38-eV excitation.

2. The 3^1D Level

The 3^1D decay scheme, which was observed via the $3^1D \rightarrow 2^1P$ (λ 6678 Å) line, is very similar to the 3^3D decay except for the relative amounts of the various cascading components. A plot of the $3^1D \rightarrow 2^1P$ decay at 34 μ after excitation with 50-eV electrons is given in Fig. 9. The 15-, 60-, and 125-nsec decay rates are identified as the lifetimes of the 3^1D, 4^1F, and 5^1F levels. The 260-nsec decay probably includes some contribution from higher n^1F levels, but the 6^1F level decay is dominant. The signal noise did not allow the detection of the next break in the decay scheme which would correspond to the ~700-nsec component in the 3^3D decay. There is considerably more 15-nsec and 60–70-nsec contribution than in the 3^3D level decay. The 15-nsec component is a larger contributor in Fig. 9 than Fig. 8 because of the larger direct-excitation cross section for the 3^1D level. The 70-nsec component is also considerably larger than in the 3^3D decay. This factor is interesting because it indicates that $4^1P \rightarrow 4^1F$ transfer is preferred to the $4^1P \rightarrow 4^3F$ transfer.

Under 100-eV excitation and at 100-μ Hg pressure, the natural 3^1D component is obscured and the nF lifetimes appear somewhat shortened as shown in Fig. 10. Further, the 4^1F lifetime appears to be shortened more than the 4^3F lifetime which was observed in the 3^3D decay under the same conditions. This would be expected if ${}^1\sigma_2 > {}^3\sigma_2$.

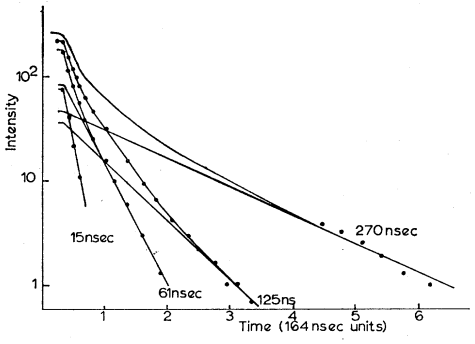

FIG. 9. Decay scheme of the 3^1D level at a pressure of 34 μ Hg after 50-eV excitation.

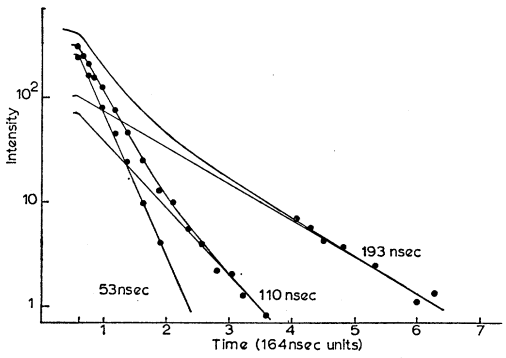

FIG. 10. Decay scheme of the 3^1D level at a pressure of 100 μ Hg after 100-eV excitation.

3. The 4^1D Level

This level was observed through the $4^1D \rightarrow 2^1P$ (λ 4922 Å) line. Only the natural lifetime (~40 nsec) and one cascading component (~130 nsec) could be extracted from the 4^1D decay schemes. The ~130-nsec decay is interpreted as the 5^1F decay. It is important to note that no 4^1P lifetimes were observed in this decay scheme. This fact supports the selection rule $\Delta L = \pm 2$ in collisional transfer from n^1P states. However, if there is a small transfer to this level, it would be difficult for us to detect it because of the poorer signal-to-noise ratio associated with this line.

4. The 3^3P Level

The decay of the 3^3P level was measured via the $3^3P \rightarrow 2^3S$ (λ 3889 Å) transition. At 100 μ Hg, the decay was found to be essentially a pure exponential with a lifetime of ~135 nsec. A natural lifetime of 115±20 nsec has been measured for this level by Pendleton and Hughes. We conclude that secondary effects are probably small; however, additional components may be present with lifetimes too near 115 nsec to be resolved.

IV. DISCUSSION

The magnitude of the back-transfer component in the n^1P decay was used to measure σ_2 for $n=5$ and $n=6$. The relative intercept of the long-lived component in the decay is a function of σ_1 and σ_2. Under the assumption that the only populating mechanism for F states is $n^1P - nF$ transfer, the density of F level atoms at $t=0$ is

$$n_f{}^0 = \rho v \sigma_1 (A_f + \rho v \sigma_2)^{-1} n_p{}^0 .$$

TABLE I. Collisional cross sections in units of 10^{-14} cm². Errors are estimated limit errors (high confidence).

	$n=4$	$n=5$	$n=6$
σ_1	2±0.2	6.4±0.7	13±2.6
σ_2	···	0.6±0.2	0.95±0.4

TABLE II. Relative and absolute contributions to the apparent 3^3D and 3^1D level excitation at 34-μ Hg pressure using interference filters for spectral isolation. Data are corrected for cascade (Sec. IIB) but are uncorrected for field of view. Also given are the branching ratios B, defined by Eq. (2.1). The cross sections are in units of 10^{-20} cm^2. Errors are limit errors.

Component lifetime (nsec)	3^3D relative contribution at 38 eV (%)	3^3D component "cross section" at 38 eV	3^1D relative contribution at 50 eV (%)	3^1D component "cross section" at 50 eV	3^3D cascade component "cross section" corrected to 50 eV	$B=Q'(n^3F\rightarrow 3^3D)/Q'(n^1F\rightarrow 3^1D)$ at 50 eV
15 ($3D$)	24±10	28	41±10	42		
70 ($4F$)	9± 6	10± 7	30±10	30±10	15±10	0.5±0.35 ($n=4$)
140 ($5F$)	17± 7	20± 8	13± 5	13± 5	30±12	2.3±1.0 ($n=5$)
260 ($6F$)	29±10	34±11	17± 8	17± 8	51±16	3.0±1.6 ($n=6$)
700 $^{nF}_{n>6}$	21±10	25±11	···	···	37±16	···

With this initial condition, the relative m^+ intercept (X_F) from (2.5) is

$$X_F=C_2(C_1+C_2)^{-1}=\rho^2v^2\sigma_1\sigma_2(A_f+\rho v\sigma_2)^{-1}(m^+-m^-)^{-1}.$$

Since σ_1 is independently determined from the slope of the m^- component decay, then σ_2 can be uniquely determined from X_F measurements. This is a much more effective way of determining σ_2 than trying to obtain it from the slope of the decays which are not particularly sensitive to σ_2. The σ_1 and σ_2 cross sections are listed on Table I for $n=4$, 5, and 6. It is found experimentally that back transfer components at $n=4$ are very small (Sec. III). The σ_2 values are in good agreement with the detailed balance argument [Eq. (2.2)] which predicts $\sigma_2\approx 0.1\sigma_1$.

The branching ratio of ^1P transfer to ^3F and ^1F levels can be inferred from the 3^3D and 3^1D decay analysis at the same electron-impact energy and pressure. However, it was found that the best experimental decay analysis was obtained under 38-eV impact and 50-eV impact for the 3^3D and 3^1D decays, respectively. It was decided to use two different energies and apply the necessary corrections for comparison at the same energy.

The 3^3D and 3^1D decay schemes produced by 38- and 50-eV electron-impact excitation, respectively, at 34-μ Hg pressure were carefully analyzed. The contributions could be placed on an absolute basis by using the absolute cross sections for 3^3D and 3^1D excitation by direct electron impact which were obtained from Ref. 11. The 15-nsec component intercepts at $t=0$ were normalized to these absolute cross section values after first making the cascade correction (Sec. IIB) to the intercepts. This procedure allowed us to place the contribution of each component to the apparent $3D$ cross section on an absolute basis. In order to compare the contribution of the cascading components ($\tau>15$ nsec) in the 3^3D decay to the 3^1D decay, the contributions of the 3^3D cascading components were corrected to correspond to 50-eV impact excitation. Since the cascading components have the energy dependency of the n^1P cross sections, the values of the cascade contributions to the apparent cross section were multiplied by the ratio of $Q(4^1P)$ at 50 eV to $Q(4^1P)$ at 38-eV impact (Fig. 1). Decay curves for the 3^3D level at 38 μ Hg after 50-eV excitation verified this adjustment.

Table II gives the relative values of the cascade-corrected intercepts, the contributions to the apparent cross section at the energies at which each decay was analyzed, and the contributions to the apparent cross section for 3^3D excitation corrected to correspond to 50-eV impact. Also given is the branching ratio determined from comparing the contributions at 50 eV. Noise limited the accuracy of the measurement of the longer lived components in the 3^1D decay. As previously mentioned, the 260-nsec component may be somewhat overestimated. This component may also be overestimated in the 3^3D level but to a lesser extent. Thus, there may be some systematic error in comparing these two components.

The data in Table II show preference for $4^1P\rightarrow 4^1F$ transfer at $n=4$ and a preference for $n^1P\rightarrow n^3F$ transfer at $n>4$. A 3 to 1 branching ratio is expected in favor of ^3F state population in the event of complete LS breakdown in the F levels. It appears, therefore, that at the $n=4$ level there is only a partial breakdown, but for $n>4$ there is nearly a complete breakdown. We conclude that $B\approx\frac{1}{2}$ for $n=4$ and $B\approx 3$ for $n>4$.

It is now possible to predict the apparent cross sections for the $3D$ levels at a given electron-impact energy and pressure from knowledge of the absolute cross sections for direct electron impact of the 3^3D, 3^1D, and n^1P levels, and the $F^i(\rho)$ functions (2.20). The absolute values of the 3^3D, 3^1D, and 4^1P direct electron-impact cross sections are taken from Ref. 10. Absolute cross sections for the n^1P series are not available past $n=6$; therefore, an n^{-3} dependence for the $Q(n^1P)$ series was assumed. Such a dependence is predicted by the Born approximation in hydrogen and has been verified between $n=2$ and 6 in helium by Skerbele and Lassettre.[12]

For $n>4$, Eq. (2.19) shows that $F_n{}^i(\rho)\propto f_n(\rho)$, where $f_n(\rho)$ has the same value in either the singlet or triplet system. The function $f_n(\rho)$ was calculated using the imprisoned n^1P transition probabilities to $n=8$ and nF transition probabilities to $n=7$ which are tabulated

[12] A. M. Skerbele and E. N. Lassettre, J. Chem. Phys. **40**, 1271 (1964).

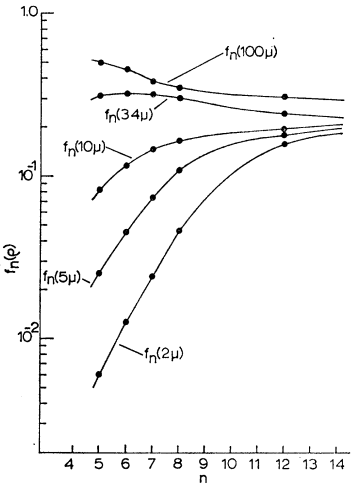

FIG. 11. The function $f_n(\rho)$ for $n \gtrsim 5$ (see text).

in Ref. 3. These transition probabilities were graphically extrapolated to $n=12$. The collisional cross sections, σ_1 and σ_2, were extrapolated using an n^4 dependence which seems to hold for the σ_1 values measured for $n=4$, 5, and 6.

Figure 11 shows the result of this extrapolation. It is to be noted that beyond $n=8$, $f_n(\rho)$ appears to be approaching a value independent of both n and ρ for pressures above 2 μ Hg. Since $\rho v\sigma_2(n) \gg A_f(n)$ for large n and pressures above 2 μ Hg and $\sigma_2(n) \approx 0.1\sigma_1(n)$, then Eq. (2.18) becomes

$$f_n(\rho) \approx A(nF \rightarrow 3D)[0.1A_p(n)+A_f(n)]^{-1}.$$

This is a slowly decreasing function with increasing n. Figure 12 was used to estimate values of $f_n(\rho)$ between $n=9$ and $n=14$. In view of expected n^{-3} decrease in $Q(n^1P)$ and very slow behavior of $f_n(\rho)$ at high n, $F_n{}^i(\rho)$ was terminated at $n=14$.

A few of the $F_n{}^i(\rho)$ are displayed in Tables III and IV for 3^1D excitation under 50-eV electron impact and 3^3D excitation under 38-eV excitation, respectively. $F_4{}^i(\rho)$ was calculated using $B=0.5$.

At a pressure of 2 μ Hg, the largest contributor to $F^i(\rho)$ is from the $n=10$ level, with all levels nearly equally contributing until at $n=14$ a definite decrease is noted. At the higher pressures where $F^i(\rho)$ begins to have values appreciable compared to unity, the largest contributors are from the $n=4$, 5, and 6 levels. For example, the contribution to $F^3(\rho)$ at 100 μ Hg from the $n=14$ level is ~ 0.01 compared to a contribution of 0.5 from the $n=5$ level.

TABLE III. Tabulation of the function $F_n{}^1(\rho)$ at 50 eV. (See text.)

	$F_n{}^1(\rho)$				
n	2 μ Hg	5 μ Hg	10 μ Hg	34 μ Hg	100 μ Hg
4	0.0039	0.0192	0.0658	0.330	0.740
5	0.0017	0.0071	0.0230	0.088	0.140
>5	0.0297	0.0523	0.0799	0.155	0.195
$F^1(\rho)$	0.0353	0.0786	0.1687	0.573	1.075

TABLE IV. Tabulation of the function $F_n{}^3(\rho)$ at 38 eV. (See text.)

	$F_n{}^3(\rho)$				
n	2 μ Hg	5 μ Hg	10 μ Hg	34 μ Hg	100 μ Hg
4	0.0019	0.0096	0.0326	0.170	0.400
5	0.0051	0.0214	0.0690	0.265	0.420
>5	0.0891	0.1569	0.2393	0.466	0.587
$F^3(\rho)$	0.0961	0.1879	0.3409	0.901	1.407

The quantity $\Omega F_n{}^i(\rho)$ gives the relative cascade from various n^iF levels to the 3^iD levels. The relative contributions of a few of the components in the $3D$ decays at 34 μ are calculated from the $F_n{}^i(\rho)$ values in Tables III and IV with $\Omega=3$ for the filter system. These contributions are compared with experimental results in Table V. The agreement is rather good.

It is interesting to compare the expected cascade contribution to the 3^3D decay at the lowest pressure at which data was taken. It was experimentally found that 68% of the 38-eV excitation at 4.3 μ Hg was due to direct excitation when the filter system was used. Using $\Omega=3$ and $F^3(5\mu)$ from Table IV, the relative amount of cascade excitation, $\Omega F^3(\rho)[1+\Omega F^3(\rho)]^{-1}$, is 36%; hence, 64% should be from direct excitation at 5 μ Hg. Extrapolating to 4.3 μ, we find 67% should be from direct excitation. The extreme agreement is probably somewhat fortuitous.

The apparent cross sections versus energy for the 3^3D and the 3^1D levels were calculated from our $F^i(\rho)$ values with $\Omega=1$, which is the case for a restricted field of view. Figures 12 and 13 show these calculations compared to the spectrometer-measured apparent cross section of St. John and Nee.[9] The values of $Q(3^1D)$ and $Q(3^3D)$ were adjusted to give the best fit at 50 and 38 eV, respectively. These values were $Q(3^1D)=34\times10^{-10}$ cm^2 and $Q(3^3D)=23\times10^{-20}$ cm^2 which necessarily must compare favorably with the corrected absolute cross sections of 36×10^{-20} cm^2 and 23×10^{-20} cm^2, respectively, found in Ref. 11.

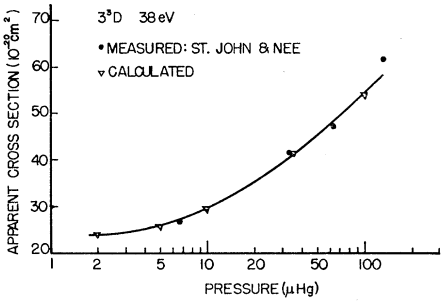

FIG. 12. Comparison of the pressure dependence of the apparent 3^3D cross section calculated using the $n^1P \rightarrow nF$ transfer model with the measurements of St. John and Nee (Ref. 9).

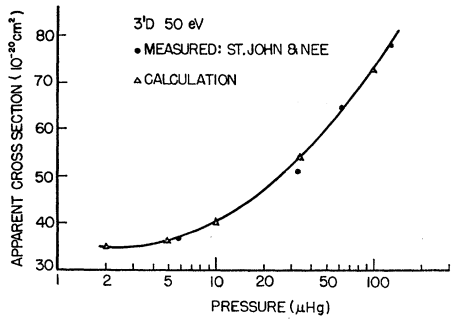

FIG. 13. Comparison of the pressure dependence of the apparent 3^1D cross section calculated using the $n^1P \rightarrow nF$ transfer model with the measurements of St. John and Nee (Ref. 9).

Our calculations assume an imprisonment radius of 1.3 cm which determines the pressure dependence of the n^1P imprisoned lifetimes. It is probable that the imprisonment radius of the apparatus of St. John and Nee will be different. However, we have determined that the calculation is rather insensitive to this parameter. While it is true that at low pressures a change by a factor of 2 in the imprisoned radius will change the imprisoned lifetime by at least a factor of 2, the total contribution of $F^i(\rho)$ to the apparent cross section at low pressures is very small. At high pressures ($\sim$100 μ Hg), on the other hand, the term in $f_n(\rho)$ including A_p is smaller than the term $A_f(\rho v \sigma_1)$ and hence a change in A_p has little effect on the results. The largest effect would be near the intermediate pressures ($\sim$35 μ Hg) where a smaller imprisonment radius would lower the value of $F^i(\rho)$ somewhat. This effect would be more noticeable for lower n. The 3^1D receives the largest share of 4^1P transfer via the 4^1F state. Hence, the effect of a different imprisonment radius would be evidenced most strongly in the 3^1D results. One notices that there is a slight disagreement at 35 μ Hg between the calculated and measured 3^1D apparent cross section presented in Fig. 13 which may be caused by a difference in imprisonment radius.

TABLE V. Comparison of measured and calculated $3D$ level decay constituents at 34-μ Hg in percent.

Lifetime of components	3^3D (38 eV) Measurement	3^3D (38 eV) Calculation	3^1D (50 eV) Measurement	3^1D (50 eV) Calculation
15	24±10	27	41±10	37
70	9± 6	13	30±10	36
140	17± 7	22	13± 5	10
250 up	50±15	37	17± 8	17

V. CONCLUSION

We feel that this work shows the validity of the $n^1P \rightarrow nF$ transfer model. We find that there is a partial breakdown in LS coupling and that the Wigner spin rule is only partially obeyed at the $n=4$ level. For $n>4$, the spin rule appears invalid, although the breakdown may not be complete until $n=6$.

For $n>4$, the cross section for $nF \rightarrow n^1P$ transfer is found to be much smaller than the reverse process. This result is consistent with the theory of detailed balancing. The magnitudes of the $n^1P \rightarrow nF$ cross section appear to increase as n^4. Such a dependency on n might be expected. For high n, the helium atom becomes hydrogenic. The excited atom becomes much larger than its ground-state collision partner and the collision cross sections go as n^4.

The long-lived components in the low pressure ($\sim$5 μ Hg) decay of the $3D$ levels can be completely attributed to collisionally populated F levels.

Finally, the pressure dependency of experimentally observed apparent $3D$ cross sections can be reproduced by calculations using the $n^1P \rightarrow nF$ transfer model, our measured collision cross sections, and our branching ratios.